

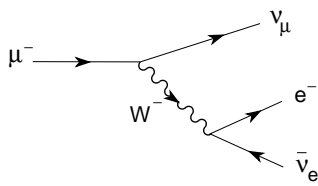
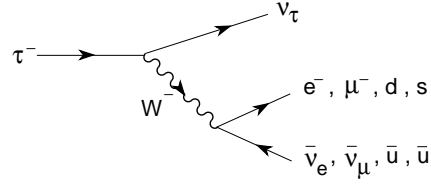
FTUV/98-16
IFIC/98-16ELECTROWEAK PRECISION PHYSICS ^a

A. PICH

*Departament de Física Teòrica, IFIC, Universitat de València - CSIC,
Dr. Moliner 50, E-46100 Burjassot, València, Spain*

Precision measurements of electroweak observables provide stringent tests of the Standard Model structure and an accurate determination of its parameters. A brief overview of the present experimental status is presented. A more extensive discussion can be found in Ref. 1.

1 Leptonic Charged-Current Couplings

Figure 1: μ -decay diagram.Figure 2: τ -decay diagram.

The simplest flavour-changing process is the leptonic decay of the μ , which proceeds through the W -exchange diagram shown in Figure 1. The momentum transfer carried by the intermediate W is very small compared to M_W . Therefore, the vector-boson propagator reduces to a contact interaction. The decay can then be described through an effective local 4-fermion Hamiltonian,

$$\mathcal{H}_{\text{eff}} = \frac{G_F}{\sqrt{2}} [\bar{e}\gamma^\alpha(1 - \gamma_5)\nu_e] [\bar{\nu}_\mu\gamma_\alpha(1 - \gamma_5)\mu], \quad \frac{G_F}{\sqrt{2}} = \frac{g^2}{8M_W^2}. \quad (1)$$

The Fermi coupling constant G_F is fixed by the total decay width,

$$\frac{1}{\tau_\mu} = \Gamma(\mu^- \rightarrow e^-\bar{\nu}_e\nu_\mu) = \frac{G_F^2 m_\mu^5}{192\pi^3} (1 + \delta_{\text{RC}}) f(m_e^2/m_\mu^2), \quad (2)$$

where $f(x) = 1 - 8x + 8x^3 - x^4 - 12x^2 \ln x$, and $\delta_{\text{RC}} = -0.0042$ takes into account the leading higher-order corrections.^{2,3} The measured μ lifetime,⁴ $\tau_\mu = (2.19703 \pm 0.00004) \times 10^{-6}$ s, implies the value

$$G_F = (1.16639 \pm 0.00002) \times 10^{-5} \text{ GeV}^{-2} \approx (293 \text{ GeV})^{-2}. \quad (3)$$

^aInvited talk at the International Workshop *Beyond the Standard Model: from Theory to Experiment* (València, 13–17 October 1997)

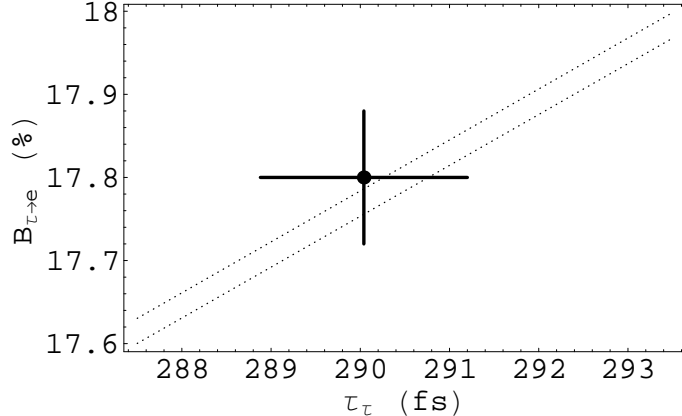


Figure 3: Relation between $B_{\tau \rightarrow e}$ and τ_τ . The dotted band corresponds to Eq. (4).

The leptonic τ decay widths $\tau^- \rightarrow e^- \bar{\nu}_e \nu_\tau, \mu^- \bar{\nu}_\mu \nu_\tau$ are also given by Eq. (2), making the appropriate changes for the masses of the initial and final leptons. Using the value of G_F measured in μ decay, one gets a relation between the τ lifetime and the leptonic branching ratios:⁵

$$B_{\tau \rightarrow e} = \frac{B_{\tau \rightarrow \mu}}{0.972564 \pm 0.000010} = \frac{\tau_\tau}{(1.6321 \pm 0.0014) \times 10^{-12} \text{ s}}. \quad (4)$$

The errors reflect the present uncertainty of 0.3 MeV in the value of m_τ .

The predicted $B_{\tau \rightarrow \mu}/B_{\tau \rightarrow e}$ ratio is in perfect agreement with the measured value $B_{\tau \rightarrow \mu}/B_{\tau \rightarrow e} = 0.972 \pm 0.007$. As shown in Figure 3, the relation between $B_{\tau \rightarrow e}$ and τ_τ is also well satisfied by the present data. These measurements test the universality of the W couplings to the leptonic charged currents. Allowing the coupling g to depend on the considered lepton flavour (i.e. g_e, g_μ, g_τ), the $B_{\tau \rightarrow \mu}/B_{\tau \rightarrow e}$ ratio constrains $|g_\mu/g_e|$, while $B_{\tau \rightarrow e}/\tau_\tau$ provides information on $|g_\tau/g_\mu|$. The present results^{1,5} are shown in Tables 1 and 2, together with the values obtained from the ratios $R_{\pi \rightarrow e/\mu} \equiv \Gamma(\pi^- \rightarrow e^- \bar{\nu}_e)/\Gamma(\pi^- \rightarrow \mu^- \bar{\nu}_\mu)$ and $R_{\tau/P} \equiv \Gamma(\tau^- \rightarrow \nu_\tau P^-)/\Gamma(P^- \rightarrow \mu^- \bar{\nu}_\mu)$ [$P = \pi, K$], from the comparison of the $\sigma \cdot B$ partial production cross-sections for the various $W^- \rightarrow l^- \bar{\nu}_l$ decay modes at the $p\bar{p}$ colliders, and from the most recent LEP2 measurements of the leptonic W^\pm branching ratios.

Although the direct constraints from the measured $W^- \rightarrow l^- \bar{\nu}_l$ branching ratios are meager, the indirect information obtained in W^\pm -mediated decays provides stringent tests of the W^\pm interactions. The present data verify the

Table 1: Present constraints on $|g_\mu/g_e|$.

	$ g_\mu/g_e $
$B_{\tau \rightarrow \mu}/B_{\tau \rightarrow e}$	0.9997 ± 0.0037
$R_{\pi \rightarrow e/\mu}$	1.0017 ± 0.0015
$\sigma \cdot B_{W \rightarrow \mu/e} \text{ (} p\bar{p} \text{)}$	0.98 ± 0.03
$B_{W \rightarrow \mu/e} \text{ (LEP2)}$	0.92 ± 0.08

 Table 2: Present constraints on $|g_\tau/g_\mu|$.

	$ g_\tau/g_\mu $
$B_{\tau \rightarrow e \tau_\mu}/\tau_\tau$	1.0008 ± 0.0030
$R_{\tau/\pi}$	1.008 ± 0.008
$R_{\tau/K}$	0.997 ± 0.035
$\sigma \cdot B_{W \rightarrow \tau/\mu} \text{ (} p\bar{p} \text{)}$	1.02 ± 0.05
$B_{W \rightarrow \tau/\mu} \text{ (LEP2)}$	1.18 ± 0.11

universality of the leptonic charged–current couplings to the 0.15% (μ/e) and 0.30% (τ/μ) level. The precision of the most recent τ –decay measurements is becoming competitive with the more accurate π –decay determination. It is important to realize the complementarity of the different universality tests. The pure leptonic decay modes probe the charged–current couplings of a transverse W . In contrast, the decays $\pi/K \rightarrow l\bar{\nu}$ and $\tau \rightarrow \nu_\tau \pi/K$ are only sensitive to the spin–0 piece of the charged current; thus, they could unveil the presence of possible scalar–exchange contributions with Yukawa–like couplings proportional to some power of the charged–lepton mass.

1.1 Lorentz Structure

Let us consider the leptonic decay $l^- \rightarrow \nu_l l' \bar{\nu}_{l'}$. The most general, local, derivative–free, lepton–number conserving, four–lepton interaction Hamiltonian, consistent with locality and Lorentz invariance^{6–10}

$$\mathcal{H} = 4 \frac{G_{l'l}}{\sqrt{2}} \sum_{n,\epsilon,\omega} g_{\epsilon\omega}^n \left[\overline{l'_\epsilon} \Gamma^n (\nu_{l'})_\sigma \right] \left[\overline{(\nu_l)_\lambda} \Gamma_n l_\omega \right], \quad (5)$$

contains ten complex coupling constants or, since a common phase is arbitrary, nineteen independent real parameters. The subindices $\epsilon, \omega, \sigma, \lambda$ label the chiralities (left–handed, right–handed) of the corresponding fermions, and n the type of interaction: scalar (I), vector (γ^μ), tensor ($\sigma^{\mu\nu}/\sqrt{2}$). For given

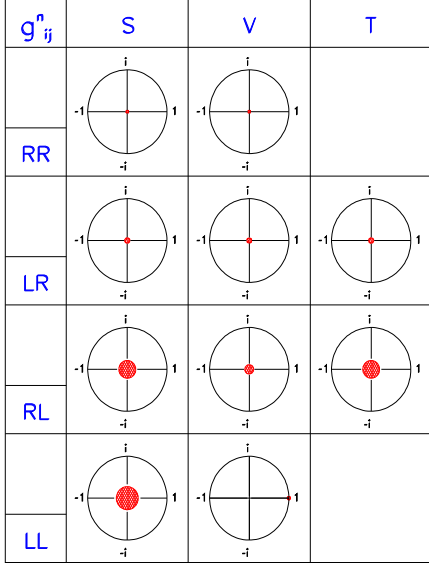


Figure 4: 90% CL experimental limits⁴ for the normalized μ -decay couplings $g_{\epsilon\omega}^n \equiv g_{\epsilon\omega}^n/N^n$.

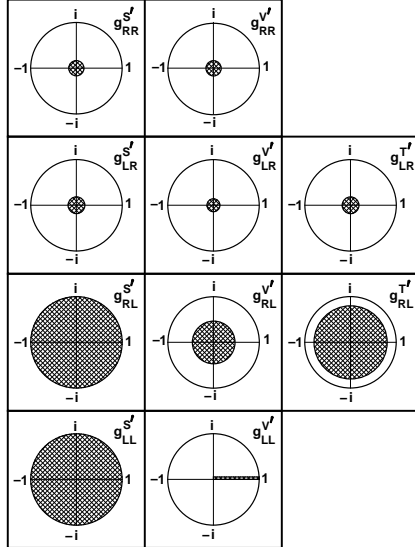


Figure 5: 90% CL experimental limits¹¹ for the normalized τ -decay couplings $g_{\epsilon\omega}^n \equiv g_{\epsilon\omega}^n/N^n$, assuming e/μ universality.

n, ϵ, ω , the neutrino chiralities σ and λ are uniquely determined. Taking out a common factor G_{Vl} , which is determined by the total decay rate, the coupling constants $g_{\epsilon\omega}^n$ are normalized to⁹

$$1 = \sum_{n, \epsilon, \omega} |g_{\epsilon\omega}^n/N^n|^2, \quad (6)$$

where $N^n = 2, 1, 1/\sqrt{3}$ for $n = S, V, T$. In the Standard Model (SM), $g_{LL}^V = 1$ and all other $g_{\epsilon\omega}^n = 0$.

The couplings $g_{\epsilon\omega}^n$ can be investigated through the measurement of the final charged-lepton distribution and with the inverse decay $\nu_l l \rightarrow l' \nu_{l'}$. For μ decay, where precise measurements of the polarizations of both μ and e have been performed, there exist⁴ stringent bounds on the couplings involving right-handed helicities. These limits show nicely that the μ -decay transition amplitude is indeed of the predicted V-A type: $|g_{LL}^V| > 0.96$ (90% CL).

Figure 5 shows the most recent limits on the τ couplings.¹¹ The measurement of the τ polarization allows to bound those couplings involving an initial right-handed lepton; however, information on the final charged-lepton

polarization is still lacking. The measurement of the inverse decay $\nu_\tau l \rightarrow \tau \nu_l$, needed to separate the g_{LL}^S and g_{LL}^V couplings, looks far out of reach.

2 Neutral–Current Couplings

In the SM, all fermions with equal electric charge have identical vector, $v_f = T_3^f(1 - 4|Q_f|\sin^2\theta_W)$ and axial–vector, $a_f = T_3^f$, couplings to the Z boson. These neutral current couplings have been precisely tested at LEP and SLC.¹²

The gauge sector of the SM is fully described in terms of only four parameters: g , g' , and the two constants characterizing the scalar potential. We can trade these parameters by^{4,12} α , G_F ,

$$M_Z = (91.1867 \pm 0.0020) \text{ GeV}, \quad (7)$$

and M_H ; this has the advantage of using the 3 most precise experimental determinations to fix the interaction. The relations

$$M_W^2 s_W^2 = \frac{\pi\alpha}{\sqrt{2}G_F}, \quad s_W^2 = 1 - \frac{M_W^2}{M_Z^2}, \quad (8)$$

determine then $s_W^2 \equiv \sin^2\theta_W = 0.2122$ and $M_W = 80.94$ GeV; in reasonable agreement with the measured W mass,¹² $M_W = 80.43 \pm 0.08$ GeV.

At tree level, the partial decay widths of the Z boson are given by

$$\Gamma[Z \rightarrow \bar{f}f] = \frac{G_F M_Z^3}{6\pi\sqrt{2}} (|v_f|^2 + |a_f|^2) N_f, \quad (9)$$

where $N_l = 1$ and $N_q = N_C$. Summing over all possible final fermion pairs, one predicts the total width $\Gamma_Z = 2.474$ GeV, to be compared with the experimental value¹² $\Gamma_Z = (2.4948 \pm 0.0025)$ GeV. The leptonic decay widths of the Z are predicted to be $\Gamma_l \equiv \Gamma(Z \rightarrow l^+l^-) = 84.84$ MeV, in agreement with the measured value $\Gamma_l = (83.91 \pm 0.10)$ MeV.

Other interesting quantities are the ratios $R_l \equiv \Gamma(Z \rightarrow \text{hadrons})/\Gamma_l$ and $R_Q \equiv \Gamma(Z \rightarrow \bar{Q}Q)/\Gamma(Z \rightarrow \text{hadrons})$. The comparison between the tree–level theoretical predictions and the experimental values, shown in Table 3, is quite good.

Additional information can be obtained from the study of the fermion–pair production process $e^+e^- \rightarrow \gamma, Z \rightarrow \bar{f}f$. LEP has provided accurate measurements of the total cross-section, the forward–backward asymmetry, the polarization asymmetry and the forward–backward polarization asymmetry:

$$\begin{aligned} \sigma^{0,f} \equiv \sigma(M_Z^2) &= \frac{12\pi}{M_Z^2} \frac{\Gamma_e \Gamma_f}{\Gamma_Z^2}, & \mathcal{A}_{\text{FB}}^{0,f} \equiv \mathcal{A}_{\text{FB}}(M_Z^2) &= \frac{3}{4} \mathcal{P}_e \mathcal{P}_f, \\ \mathcal{A}_{\text{Pol}}^{0,f} \equiv \mathcal{A}_{\text{Pol}}(M_Z^2) &= \mathcal{P}_f, & \mathcal{A}_{\text{FB,Pol}}^{0,f} \equiv \mathcal{A}_{\text{FB,Pol}}(M_Z^2) &= \frac{3}{4} \mathcal{P}_e, \end{aligned} \quad (10)$$

where Γ_f is the Z partial decay width to the $\bar{f}f$ final state, and

$$\mathcal{P}_f \equiv \frac{-2v_f a_f}{v_f^2 + a_f^2} \quad (11)$$

is the average longitudinal polarization of the fermion f .

The measurement of the final polarization asymmetries can (only) be done for $f = \tau$, because the spin polarization of the τ 's is reflected in the distorted distribution of their decay products. Therefore, \mathcal{P}_τ and \mathcal{P}_e can be determined from a measurement of the spectrum of the final charged particles in the decay of one τ , or by studying the correlated distributions between the final products of both τ' s.¹³

With polarized e^+e^- beams, one can also study the left-right asymmetry between the cross-sections for initial left- and right-handed electrons. At the Z peak, this asymmetry directly measures the average initial lepton polarization, \mathcal{P}_e , without any need for final particle identification. SLD has also measured the left-right forward-backward asymmetry for b and c quarks, which are only sensitive to the final state couplings:

$$\mathcal{A}_{\text{LR}}^0 \equiv \mathcal{A}_{\text{LR}}(M_Z^2) = -\mathcal{P}_e, \quad \mathcal{A}_{\text{FB,LR}}^{0,f} \equiv \mathcal{A}_{\text{FB,LR}}^f(M_Z^2) = -\frac{3}{4}\mathcal{P}_f. \quad (12)$$

Using $s_W^2 = 0.2122$, one gets the predictions shown in the second column of Table 3. The comparison with the experimental measurements looks reasonable for the total hadronic cross-section $\sigma_{\text{had}}^0 \equiv \sum_q \sigma^{0,q}$; however, all leptonic asymmetries disagree with the measured values by several standard deviations. As shown in the table, the same happens with the heavy-flavour forward-backward asymmetries $\mathcal{A}_{\text{FB}}^{0,b/c}$, which compare very badly with the experimental measurements; the agreement is however better for $\mathcal{P}_{b/c}$.

Clearly, the problem with the asymmetries is their high sensitivity to the input value of $\sin^2 \theta_W$; specially the ones involving the leptonic vector coupling $v_l = (1 - 4 \sin^2 \theta_W)/2$. Therefore, they are an extremely good window into higher-order electroweak corrections.

2.1 Important QED and QCD Corrections

The photon propagator gets vacuum polarization corrections, induced by virtual fermion-antifermion pairs. Their effect can be taken into account through a redefinition of the QED coupling, which depends on the energy scale of the process; the resulting effective coupling $\alpha(s)$ is called the QED *running coupling*. The fine structure constant is measured at very low energies; it corresponds to $\alpha(m_e^2)$. However, at the Z peak, we should rather use $\alpha(M_Z^2)$.

Table 3: Comparison between SM predictions and experimental¹² measurements. The third column includes the main QED and QCD corrections. The experimental value for s_W^2 refers to the effective electroweak mixing angle in the charged-lepton sector.

Parameter	Tree-level prediction		SM fit (1-loop)	Experimental value
	Naive	Improved		
M_W (GeV)	80.94	79.96	80.375	80.43 ± 0.08
s_W^2	0.2122	0.2311	0.23152	0.23152 ± 0.00023
Γ_Z (GeV)	2.474	2.490	2.4966	2.4948 ± 0.0025
R_l	20.29	20.88	20.756	20.775 ± 0.027
σ_{had}^0 (nb)	42.13	41.38	41.467	41.486 ± 0.053
$\mathcal{A}_{\text{FB}}^{0,l}$	0.0657	0.0169	0.0162	0.0171 ± 0.0010
\mathcal{P}_l	-0.296	-0.150	-0.1470	-0.1505 ± 0.0023
$\mathcal{A}_{\text{FB}}^{0,b}$	0.210	0.105	0.1031	0.0984 ± 0.0024
$\mathcal{A}_{\text{FB}}^{0,c}$	0.162	0.075	0.0736	0.0741 ± 0.0048
\mathcal{P}_b	-0.947	-0.936	-0.935	-0.900 ± 0.050
\mathcal{P}_c	-0.731	-0.669	-0.668	-0.650 ± 0.058
R_b	0.219	0.220	0.2158	0.2170 ± 0.0009
R_c	0.172	0.170	0.1723	0.1734 ± 0.0048

The long running from m_e to M_Z gives rise to a sizeable correction:^{14,15} $\alpha(M_Z^2)^{-1} = 128.896 \pm 0.090$. The quoted uncertainty arises from the light-quark contribution, which is estimated from $\sigma(e^+e^- \rightarrow \text{hadrons})$ and τ -decay data.

Since G_F is measured at low energies, while M_W is a high-energy parameter, the relation between both quantities in Eq. (8) is clearly modified by vacuum-polarization contributions. One gets then the corrected predictions $M_W = 79.96$ GeV and $s_W^2 = 0.2311$.

The gluonic corrections to the $Z \rightarrow \bar{q}q$ decays can be directly incorporated by taking an effective number of colours $N_q = N_C \left\{ 1 + \frac{\alpha_s}{\pi} + \dots \right\} \approx 3.12$, where we have used $\alpha_s(M_Z^2) \approx 0.12$.

The third column in Table 3 shows the numerical impact of these QED and QCD corrections. In all cases, the comparison with the data gets improved. However, it is in the asymmetries where the effect gets more spectacular. Owing to the high sensitivity to s_W^2 , the small change in the value of the weak mixing angle generates a huge difference of about a factor of 2 in the predicted asymmetries. The agreement with the experimental values is now very good.

2.2 Higher-Order Electroweak Corrections

Initial- and final-state photon radiation is by far the most important numerical correction. One has in addition the contributions coming from photon exchange between the fermionic lines. All these QED corrections are to a large extent dependent on the detector and the experimental cuts, because of the infra-red problems associated with massless photons. These effects are usually estimated with Monte Carlo programs and subtracted from the data.

More interesting are the so-called *oblique* corrections, gauge-boson self-energies induced by vacuum polarization diagrams, which are *universal* (process independent). In the case of the W^\pm and the Z , these corrections are sensitive to heavy particles (such as the top) running along the loop.¹⁶ In QED, the vacuum polarization contribution of a heavy fermion pair is suppressed by inverse powers of the fermion mass. At low energies ($s \ll m_f^2$), the information on the heavy fermions is then lost. This *decoupling* of the heavy fields happens in theories like QED and QCD, with only vector couplings and an exact gauge symmetry.¹⁷ The SM involves, however, a broken chiral gauge symmetry. The W^\pm and Z self-energies induced by a heavy top generate contributions which increase quadratically with the top mass.¹⁶ The leading m_t^2 contribution to the W^\pm propagator amounts to a -3% correction to the relation (8) between G_F and M_W .

Owing to an accidental $SU(2)_C$ symmetry of the scalar sector, the virtual production of Higgs particles does not generate any m_H^2 dependence at one loop.¹⁶ The dependence on the Higgs mass is only logarithmic. The numerical size of the correction induced on (8) is -0.3% ($+1\%$) for $m_H = 60$ (1000) GeV.

The vertex corrections are *non-universal* and usually smaller than the oblique contributions. There is one interesting exception, the $Z\bar{b}b$ vertex, which is sensitive to the top quark mass.¹⁸ The $Z\bar{f}f$ vertex gets 1-loop corrections where a virtual W^\pm is exchanged between the two fermionic legs. Since, the W^\pm coupling changes the fermion flavour, the decays $Z \rightarrow \bar{d}_i \bar{d}_i$ get contributions with a top quark in the internal fermionic lines. These amplitudes are suppressed by a small quark-mixing factor $|V_{td_i}|^2$, except for the $Z \rightarrow \bar{b}b$ vertex because $|V_{tb}| \approx 1$. The explicit calculation¹⁸⁻²¹ shows the presence of hard m_t^2 corrections to the $Z \rightarrow \bar{b}b$ vertex, which amount to a -1.5% effect in $\Gamma(Z \rightarrow \bar{b}b)$.

The *non-decoupling* present in the $Z\bar{b}b$ vertex is quite different from the one happening in the boson self-energies. The vertex correction does not have any dependence with the Higgs mass. Moreover, while any kind of new heavy particle, coupling to the gauge bosons, would contribute to the W^\pm and Z self-energies, possible new-physics contributions to the $Z\bar{b}b$ vertex are much more

restricted and, in any case, different. Therefore, an independent experimental test of the two effects is very valuable in order to disentangle possible new-physics contributions from the SM corrections.

The remaining quantum corrections (box diagrams, Higgs exchange) are rather small at the Z peak.

2.3 Lepton Universality

Table 4: Measured values¹² of Γ_l and the leptonic forward–backward asymmetries. The last column shows the combined result (for a massless lepton) assuming lepton universality.

	e	μ	τ	l
Γ_l (MeV)	83.94 ± 0.14	83.84 ± 0.20	83.68 ± 0.24	83.91 ± 0.10
$\mathcal{A}_{\text{FB}}^{0,l}$ (%)	1.60 ± 0.24	1.63 ± 0.14	1.92 ± 0.18	1.71 ± 0.10

Table 5: Measured values¹² of the leptonic polarization asymmetries.

$-\mathcal{A}_{\text{Pol}}^{0,\tau} = -\mathcal{P}_\tau$	$-\frac{4}{3}\mathcal{A}_{\text{FB,Pol}}^{0,\tau} = -\mathcal{P}_e$	$\mathcal{A}_{\text{LR}}^0 = -\mathcal{P}_e$	$\{\frac{4}{3}\mathcal{A}_{\text{FB}}^{0,l}\}^{1/2} = -P_l$
0.1411 ± 0.0064	0.1399 ± 0.0073	0.1547 ± 0.0032	0.1510 ± 0.0044

Tables 4 and 5 show the present experimental results for the leptonic Z decay widths and asymmetries. The data are in excellent agreement with the SM predictions and confirm the universality of the leptonic neutral couplings. There is however a small 1.9σ discrepancy between the \mathcal{P}_e values obtained¹² from $\mathcal{A}_{\text{FB,Pol}}^{0,\tau}$ and $\mathcal{A}_{\text{LR}}^0$. The average of the two τ polarization measurements, $\mathcal{A}_{\text{Pol}}^{0,\tau}$ and $\frac{4}{3}\mathcal{A}_{\text{FB,Pol}}^{0,\tau}$, results in $\mathcal{P}_l = -0.1406 \pm 0.0048$ which disagrees with the $\mathcal{A}_{\text{LR}}^0$ measurement at the 2.4σ level. Assuming lepton universality, the combined result from all leptonic asymmetries gives

$$\mathcal{P}_l = -0.1505 \pm 0.0023 \quad (\chi^2/\text{d.o.f.} = 6.0/2) . \quad (13)$$

Figure 6 shows the 68% probability contours in the a_l – v_l plane, obtained from a combined analysis¹² of all leptonic observables.

The neutrino couplings can be determined from the invisible Z –decay width, $\Gamma_{\text{inv}}/\Gamma_l = 5.960 \pm 0.022$, by assuming three identical neutrino generations with left–handed couplings and fixing the sign from neutrino scattering data.²² The resulting experimental value,¹² $v_\nu = a_\nu = 0.50125 \pm 0.00092$, is in perfect agreement with the SM. Alternatively, one can use the SM prediction, $\Gamma_{\text{inv}}/\Gamma_l = (1.991 \pm 0.001) N_\nu$, to get a determination of the number of (light)

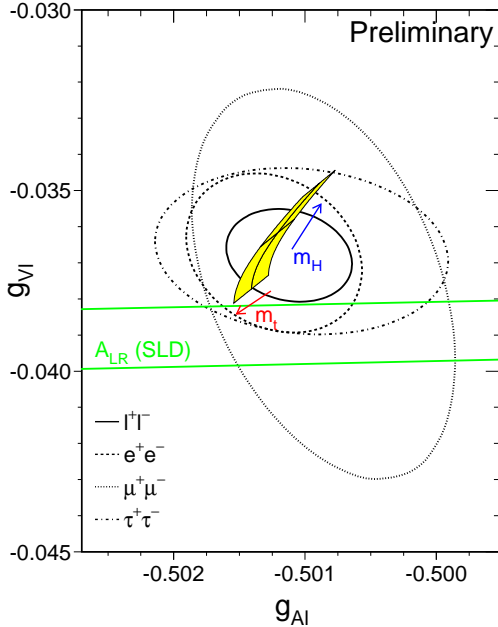


Figure 6: 68% probability contours in the a_l - v_l plane from LEP measurements.¹² The solid contour assumes lepton universality. Also shown is the 1σ band resulting from the A_{LR}^0 measurement at SLD. The shaded region corresponds to the SM prediction for $m_t = 175.6 \pm 5.5$ GeV and $m_H = 300^{+700}_{-240}$ GeV.

neutrino flavours:¹²

$$N_\nu = 2.993 \pm 0.011. \quad (14)$$

The universality of the neutrino couplings has been tested with $\nu_\mu e$ scattering data, which fixes²³ the ν_μ coupling to the Z : $v_{\nu_\mu} = a_{\nu_\mu} = 0.502 \pm 0.017$.

Assuming lepton universality, the measured leptonic asymmetries can be used to obtain the effective electroweak mixing angle in the charged-lepton sector:

$$\sin^2 \theta_{\text{eff}}^{\text{lept}} \equiv \frac{1}{4} \left(1 - \frac{v_l}{a_l} \right) = 0.23109 \pm 0.00029. \quad (15)$$

Including also the information provided by the hadronic asymmetries, one gets¹² $\sin^2 \theta_{\text{eff}}^{\text{lept}} = 0.23152 \pm 0.00023$ with a $\chi^2/\text{d.o.f.} = 12.5/6$.

Table 6: Results from the global electroweak fits¹² to LEP data alone, to all data except the direct measurements of m_t and M_W at Tevatron and LEP2, and to all data.

	LEP only (M_W included)	All data except m_t and M_W	All data
m_t (GeV)	158^{+14}_{-11}	157^{+10}_{-9}	173.1 ± 5.4
m_H (GeV)	83^{+168}_{-49}	41^{+64}_{-21}	115^{+116}_{-66}
$\log(m_H)$	$1.92^{+0.48}_{-0.39}$	$1.62^{+0.41}_{-0.31}$	$2.06^{+0.30}_{-0.37}$
$\alpha_s(M_Z^2)$	0.121 ± 0.003	0.120 ± 0.003	0.120 ± 0.003
$\chi^2/\text{d.o.f.}$	8/9	14/12	17/15
$\sin^2 \theta_{\text{eff}}^{\text{lept}}$	0.23188 ± 0.00026	0.23153 ± 0.00023	0.23152 ± 0.00022
$1 - M_W^2/M_Z^2$	0.2246 ± 0.0008	0.2240 ± 0.0008	0.2231 ± 0.0006
M_W (GeV)	80.298 ± 0.043	80.329 ± 0.041	80.375 ± 0.030

2.4 SM Electroweak Fit

The high accuracy of the present data provides compelling evidence for the pure weak quantum corrections, beyond the main QED and QCD corrections discussed in Section 2.1. The measurements are sufficiently precise to require the presence of quantum corrections associated with the virtual exchange of top quarks, gauge bosons and Higgses.

Table 6 shows the constraints obtained on m_t , m_H and $\alpha_s(M_Z^2)$, from a global fit to the electroweak data.¹² The bottom part of the table lists derived results for $\sin^2 \theta_{\text{eff}}^{\text{lept}}$, $1 - M_W^2/M_Z^2$ and M_W . Three different fits are shown. The first one uses only LEP data, including the LEP2 determination of M_W . The fitted value of the top mass is in good agreement with the Tevatron measurement,¹² $m_t = 175.6 \pm 5.5$ GeV, although slightly lower. The data seems to prefer also a light Higgs. There is a large correlation (0.76) between the fitted values of m_t and m_H ; the correlation would be much larger if the R_b measurement was not used (R_b is insensitive to m_H). The extracted value of the strong coupling agrees very well with the world average value⁴ $\alpha_s(M_Z^2) = 0.118 \pm 0.003$.

The second fit includes all electroweak data except the direct measurements of m_t and M_W , performed at Tevatron and LEP2. The fitted values for these two masses agree well with the direct determinations. The indirect measurements clearly prefer low m_t and low m_H . The best constraints on m_H are obtained in the last fit, which includes all available data. Taking into account additional theoretical uncertainties due to missing higher-order corrections,

the global fit results in the upper bound:¹²

$$m_H < 420 \text{ GeV} \quad (95\% \text{ CL}) . \quad (16)$$

The uncertainty on $\alpha(M_Z^2)^{-1}$ introduces a severe limitation on the accuracy of the SM predictions. To improve the present determination of $\alpha(M_Z^2)^{-1}$ one needs to perform a good measurement of $\sigma(e^+e^- \rightarrow \text{hadrons})$, as a function of the centre-of-mass energy, in the whole kinematical range spanned by DAΦNE, a tau-charm factory and the B factories. This would result in a much stronger constraint on the Higgs mass.

This work has been supported in part by CICYT (Spain) under grant No. AEN-96-1718.

References

1. A. Pich, *Precision Tests of the Standard Model*, Proc. XXV International Winter Meeting on Fundamental Physics (Formigal, 3–8 March 1997), ed. E. Fernández (World Scientific, Singapore, 1998) [hep-ph/9711279].
2. T. Kinoshita and A. Sirlin, *Phys. Rev.* **113** (1959) 1652.
3. W.J. Marciano and A. Sirlin, *Phys. Rev. Lett.* **61** (1988) 1815.
4. Particle Data Group, *Review of Particle Properties*, *Phys. Rev.* **D54** (1996) 1; and 1997 update [<http://pdg.lbl.gov/>].
5. A. Pich, *Nucl. Phys. B (Proc. Suppl.)* **55C** (1997) 3.
6. L. Michel, *Proc. Phys. Soc.* **A63** (1950) 514; 1371.
7. C. Bouchiat and L. Michel, *Phys. Rev.* **106** (1957) 170.
8. T. Kinoshita and A. Sirlin, *Phys. Rev.* **107** (1957) 593; **108** (1957) 844.
9. W. Fettscher *et al*, *Phys. Lett.* **B173** (1986) 102.
10. A. Pich and J.P. Silva, *Phys. Rev.* **D52** (1995) 4006.
11. J.P. Alexander *et al* (CLEO), *Phys. Rev.* **D56** (1997) 5320.
12. The LEP Collaborations ALEPH, DELPHI, L3, OPAL, the LEP Electroweak Working Group and the SLD Heavy Flavour Group, *A Combination of Preliminary Electroweak Measurements and Constraints on the Standard Model*, CERN preprint CERN-PPE/97-154 (December 1997).
13. R. Alemany *et al*, *Nucl. Phys.* **B379** (1992) 3.
14. M. Davier and A. Höcker, hep-ph/9801361.
15. S. Eidelmann and F. Jegerlehner, *Z. Phys.* **C67** (1995) 585.
16. M. Veltman, *Nucl. Phys.* **B123** (1977) 89.
17. T. Appelquist and J. Carazzone, *Phys. Rev.* **D11** (1975) 2856.
18. J. Bernabéu, A. Pich and A. Santamaría, *Phys. Lett.* **B200** (1988) 569; *Nucl. Phys.* **B363** (1991) 326.

19. A.A. Akhundov *et al*, *Nucl. Phys.* **B276** (1986) 1.
20. W. Beenakker and W. Hollik, *Z. Phys.* **C40** (1988) 141.
21. B.W. Lynn and R.G. Stuart, *Phys. Lett.* **B252** (1990) 676.
22. P. Vilain *et al* (CHARM II), *Phys. Lett.* **B335** (1994) 246.
23. P. Vilain *et al* (CHARM II), *Phys. Lett.* **B320** (1994) 203.